



**HAL**  
open science

# Numerical simulation of the dynamics of an impacting bar

Laetitia Paoli, Michelle Schatzman

► **To cite this version:**

Laetitia Paoli, Michelle Schatzman. Numerical simulation of the dynamics of an impacting bar. *Computer Methods in Applied Mechanics and Engineering*, 2007, 196 (29-30), pp.2839 - 2851. 10.1016/j.cma.2006.11.024 . hal-01635192

**HAL Id: hal-01635192**

**<https://hal.science/hal-01635192>**

Submitted on 14 Nov 2017

**HAL** is a multi-disciplinary open access archive for the deposit and dissemination of scientific research documents, whether they are published or not. The documents may come from teaching and research institutions in France or abroad, or from public or private research centers.

L'archive ouverte pluridisciplinaire **HAL**, est destinée au dépôt et à la diffusion de documents scientifiques de niveau recherche, publiés ou non, émanant des établissements d'enseignement et de recherche français ou étrangers, des laboratoires publics ou privés.

# Numerical simulation of the dynamics of an impacting bar

Laetitia Paoli <sup>a,\*</sup>, Michelle Schatzman <sup>b</sup>

<sup>a</sup> *LaMUSE (Laboratoire de Mathématiques de l'Université de Saint-Etienne), Université de Saint-Étienne,  
23 rue du Dr Paul Michelon, 42023 Saint-Étienne Cedex 2, France*

<sup>b</sup> *MAPLY, CNRS et Université Claude Bernard, Lyon 1, 69622 Villeurbanne Cedex, France*

We calculate numerically the motion of a slender bar dropped on a rigid foundation. For the computation the bar is discretized by a system of rigid bodies linked by spiral springs or by a pair of linear springs. We assume that the impact is frictionless and we model it by Newton's law. We compute the motion by using either an event-driven method based on the detection of impacts or a time-stepping scheme avoiding the detection of impacts. We calculate also the apparent restitution coefficient and we compare our results with the experimental and numerical results of Stoianovici and Hurmuzlu.

*Keywords:* Dynamics of discrete mechanical systems; Frictionless unilateral constraints; Microimpacts; Restitution coefficient; Event-driven scheme; Time-stepping scheme

## 1. Introduction

This article is devoted to the numerical calculation of motion with impact of a discrete mechanical system subject to unilateral frictionless constraints. The transmission of velocities at impacts is modelled by Newton's law: the normal impulsion is reflected and multiplied by a restitution coefficient  $e \in [0, 1]$  and the tangential impulsion is conserved.

The article contains the description of two numerical methods and of their implementation. The first method is the so-called event-driven method which integrates the motion by a Newmark's scheme when the constraints are inactive and seeks the instants of impact; once these instants are found with a satisfactory precision, we apply the impact law and we start again. The event-driven method is not efficient, but we trust its numerical results and use it as a reference.

The second method is a time-stepping scheme, which avoids the detection of the instants of impact and therefore is faster than the previous one. For impacting systems modelled by unilateral rigid and frictionless constraints, the convergence of this scheme has been proved for an arbitrary coefficient of restitution; see [1,2]; when the mass matrix is not constant, this scheme is probably the only one for which a convergence proof is known.

It could be easily argued that the second method is not very precise—which is true—but since the class of problems with impact is usually very sensitive to initial data, it is quite possible that the trajectorywise precision is less reassuring than a good old proof *cum* estimates.

We compare the time-stepping scheme to the event-driven method on specific examples.

We have chosen an application which allowed comparison to experiments, viz. the experiments described by Hurmuzlu and Stoianovici [3] and by Hurmuzlu [4]. Consider indeed a thin cylindrical bar whose impacting end is shaped as a half-sphere. Initially, the bar makes an angle  $\theta$  with the horizontal; the bar is dropped onto a rigid foundation, bounces back and the apparent restitution coefficient of

---

\* Corresponding author. Tel.: +33 4 77 48 15 42; fax: +33 4 77 25 60 71.  
*E-mail address:* laetitia.paoli@univ-st-etienne.fr (L. Paoli).

the impacting degree of freedom is measured. The motion is planar.

This model is interesting for several reasons; first the coefficient of restitution is a rather ill-defined concept, as this set of experiments definitively proved: the apparent coefficient of restitution as observed by Hurmuzlu and Stoianovici depends very strongly on the initial angle of the bar with the horizontal. Therefore, knowing whether our scheme will simulate this behavior is an interesting question, all the more because our model of impact uses a coefficient of restitution. Second, the mass matrix in our beam models is not trivial for reasonable generalized coordinates. Third, the articles of Stoianovici and Hurmuzlu include some computations based on normal compliance models, and therefore, it is nice to compare our results to their calculations.

Indeed, the observation that the apparent restitution coefficient depends strongly on the angle  $\theta$  is the consequence of the interaction between the continuous medium mode and the impact. This interaction has been explained in [3,4], and a mathematical argument based on asymptotics has been given in [5]. The reader will observe that the results of our simulations are quite comparable to the above-mentioned experimental results.

The reader may wonder why we kept to a restitution coefficient model, while in the same time these experiments radically nullify that concept. The reason is that, experimentally, as we shall show, the simulations corresponding to different numerical coefficients of restitution are quite close, and moreover, the energy loss implied by the shock law concerns only a small part of the energy, since the bar is discretized into elements. Therefore, the influence of this choice can be reasonably thought to tend to 0 as the size of the elements tends to 0. In other words, the numerical discretization of a continuous medium by our methods is rather indifferent to the detailed shock law we have chosen in order to perform the time integration, but however, our simulations retain the physics of the phenomenon.

Let us mention that we used two different discretizations of the bar for the following reason: the model with spiral springs seems more natural to us from the mechanical point of view; however, the model with pairs of spring is basically the same as the one used by Stoianovici and Hurmuzlu [3], who, however, employed a normal compliance model of the impact. Since we wanted to compare our results with their calculations and with their experiments, we needed to take a model of the beam which was as close as possible to their model.

The implementation and numerical results for model 1 have been briefly described in [7], which appeared as a CD-ROM, and even more concisely in [2]. The implementation and the numerical results for model 2 have never been published.

It is reasonable to ask whether we could have used instead of a rigid contact a compliant contact, also known as a penalty method. In some cases, such as those treated by Stronge [6], it is feasible to get values for the compliance, and then, to integrate the corresponding system of

differential equations with the help of a standard O.D.E. integration package, such as can be found in MATLAB or SCILAB. In the most common situations, we have no reasonable estimate of the compliance. If the solution depended strongly on the compliance coefficient, it would not be a good option to calculate a numerical solution through a compliant approximation. Stating that the solution does not depend strongly on the compliance coefficient, as it tends to infinity, is a way of stating in practical terms a convergence theorem, and we refer to [8–12] for a number of convergence results.

However, practically, we are dissatisfied with compliant approximation: they require the introduction of an extra parameter, and the numerical integration of the correspondingly very stiff systems is not terribly efficient, as compared to our time-stepping scheme. We refer the reader to [13] for a more detailed comparison of methods with rigid constraints to methods with compliant constraints.

## 2. The models

In this section, we describe the mechanics of our problem. We have chosen to treat the bar which was the object of most attention in [3]; its physical and geometrical parameters are given in Table 1.

### 2.1. The discretization of the continuous beam

We use two different mechanical models of a bar with a finite number of degrees of freedom:

- (1) The bar is discretized by a finite number  $n$  of identical cylindrical segments (of circular section) and a half-sphere at the impacting end; the nearest segment to the impacting half-sphere is joined by a linear spring; every other segment is joined to its neighbor by three springs and an articulation: two of these springs of stiffness  $k$  extend the segments, and the third is a flexion spring of stiffness  $\Gamma$  which responds linearly to the angle difference between adjoining segments. The length  $2L$  is the sum of the length of one segment and its two compression springs in the reference state. We make a simplifying assumption by imposing that the extension of the springs on either side of a beam segment is the same, and that the spiral spring is centered at the intersection of the axis of one beam segment with the axis of its neighbor. The reader is referred to Fig. 1 to see the setup. We choose as generalized coordinates for this model the coordinates  $(x_0, y_0)$  of the centre of the half-sphere, the angles  $\theta_i$

Table 1  
Geometrical and physical data

Length of the bar	0.2 m
Radius of the bar	0.00635 m
Density of the bar	7876.74 kg/m <sup>3</sup>
Young's modulus	$2.1 \times 10^{11}$ S.I. units

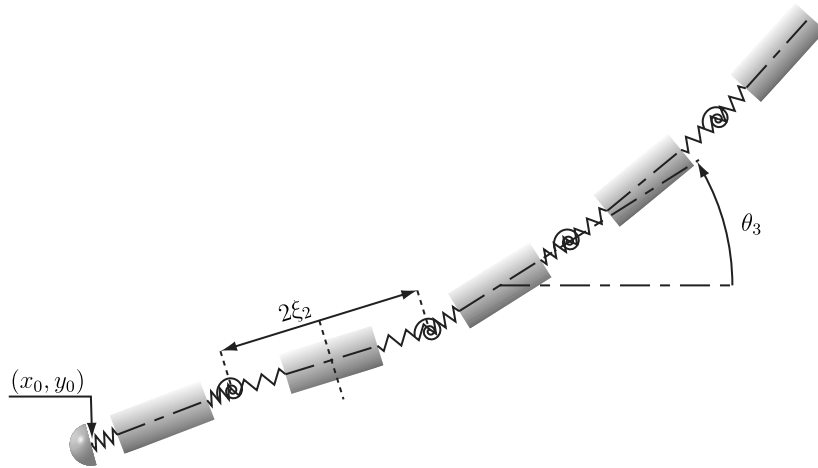


Fig. 1. The discretization of the bar in model 1 and the associated generalized coordinates.

and the lengths  $\xi_i$  shown on the figure, with the convention that  $2\xi_i$  is the sum of the length of the beam segment and of its neighboring two springs. Of course, there is different convention for the last segment, since it has a neighbor on one side only:  $\xi_n$  is the length of the half-segment plus the spring. Therefore, the extension of each spring attached to the  $i$ th segment is  $\xi_i - L$ .

- (2) In the second model, the beam is decomposed as above, and the impacting half-sphere is joined to its neighbor as previously. The other segments are joined by pairs of linear springs, which are offset by  $a/2$  away from the axes of the beam segment. All the linear springs in this model have the same stiffness  $k$ . The main geometrical assumption is that each pair of neighboring beam segments is symmetric with respect to the mediatrix of the segment between the facing extremities; see Fig. 2 to picture this assumption. Here  $2L$  is the length of the beam segment plus the length of one spring at rest. We choose as generalized coordinates  $(x_0, y_0)$  and the  $\theta_i$ 's, which have the same meaning as above, and the  $\lambda_i$  pictured at Fig. 2;  $\lambda_1$  denotes the extension the first spring; for  $i$  varying from 2 to  $n$ ,  $\lambda_i$  is as indicated on the figure.

The reader should observe that model 2 comes from [3], so as to have a truly comparable situation.

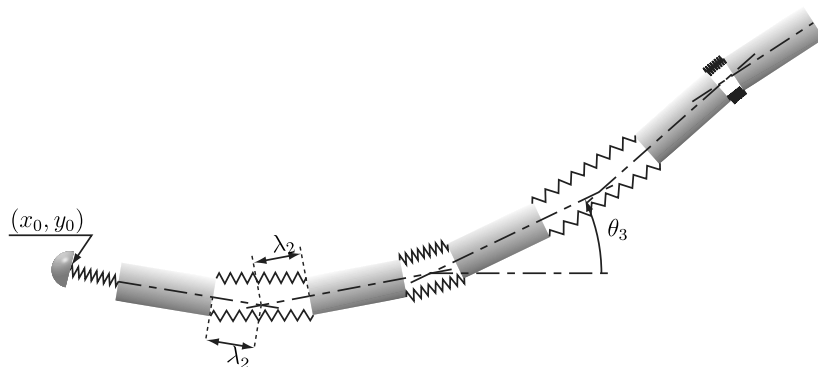


Fig. 2. The discretization of the bar in model 2 and the associated generalized coordinates.

### 2.1.1. The Lagrangian of the first model

The Lagrangian relative to the first discretization of the bar is defined as follows: the mass of each segment is  $m$ , the mass of the end hemisphere is  $\mu$ , the moment of inertia of each segment with respect to its center of gravity and the axis orthogonal to the plane of the experiment is  $I$  and the moment of inertia of the hemisphere with respect to its center (not its center of inertia!) and the axis orthogonal to the plane of the experiment is  $J$ .

The center of gravity of the  $i$ th segment has coordinates

$$x_i = x_0 + 2 \sum_{j=1}^{i-1} \xi_j \cos \theta_j + \xi_i \cos \theta_i,$$

$$y_i = y_0 + 2 \sum_{j=1}^{i-1} \xi_j \sin \theta_j + \xi_i \sin \theta_i.$$

The center of gravity of the end hemisphere has coordinates

$$x_G = x_0 - \frac{3R}{8} \cos \theta_1, \quad y_G = y_0 - \frac{3R}{8} \sin \theta_1.$$

We recall our choice of generalized coordinates:

$$q = (x_0, y_0, \theta_1, \dots, \theta_n, \xi_1, \dots, \xi_n).$$

Then the kinetic energy and the potential energy are defined respectively by

$$T = \frac{\mu}{2}(\dot{x}_G^2 + \dot{y}_G^2) + \frac{m}{2} \sum_{i=1}^n (\dot{x}_i^2 + \dot{y}_i^2) + \frac{J\dot{\theta}_1^2}{2} + \frac{I}{2} \sum_{i=1}^n \dot{\theta}_i^2, \quad (1)$$

$$U = \mu g y_G + mg \sum_{i=1}^n y_i + k \sum_{i=1}^{n-1} (\xi_i - L)^2 + \frac{k}{2} (\xi_n - L)^2 + \frac{\Gamma}{2} \sum_{i=1}^{n-1} (\theta_i - \theta_{i+1})^2. \quad (2)$$

### 2.1.2. The Lagrangian for the second model

For the second model, the coordinates of the center of mass of the  $i$ th segment are

$$x_i = x_0 + \sum_{j=1}^{i-1} (2L + \lambda_j + \lambda_{j+1}) \cos \theta_j + (L + \lambda_i) \cos \theta_i,$$

$$y_i = y_0 + \sum_{j=1}^{i-1} (2L + \lambda_j + \lambda_{j+1}) \sin \theta_j + (L + \lambda_i) \sin \theta_i,$$

and the generalized coordinates are

$$q = (x_0, y_0, \theta_1, \dots, \theta_n, \lambda_1, \dots, \lambda_n).$$

The kinetic energy is given by Eq. (1). The potential energy is now given by

$$U = \mu g y_G + mg \sum_{i=1}^n y_i + \frac{k}{2} \lambda_1^2 + \sum_{i=2}^n U_i, \quad (3)$$

where  $U_i$ , which is the elastic potential energy of the pair of springs between segments  $i-1$  and  $i$ , is given by the expression

$$U_i = 2k \left( \frac{a^2}{4} + \lambda_i^2 + \cos(\theta_i - \theta_{i-1}) \left( \lambda_i^2 - \frac{a^2}{4} \right) \right). \quad (4)$$

### 2.1.3. Computation of the mechanical parameters $k$ , $\Gamma$ and $a$

In both cases, we use the strategy of Stoianovici and Hurmuzlu's article [3]. Denote by  $E$  Young's modulus of the material, by  $R$  the radius of the bar. Then, for the first model, the stiffness  $k$  is given by

$$k = \frac{E\pi R^2}{3nL} \frac{(n-1)(3n-1)}{n},$$

and the value of  $\Gamma$  is given by

$$\Gamma = \frac{E\pi R^4}{56nL} \frac{(n-1)(7n-5)}{n}.$$

Let  $\rho$  be the volume mass of the material of the bar. The values of  $I$ ,  $J$ ,  $m$  and  $\mu$  are

$$I = m \left( \frac{L^2}{3} + \frac{R^2}{4} \right), \quad J = \frac{2\mu R^2}{5}, \quad m = 2L\pi R^2 \rho, \quad \mu = \frac{2\rho\pi R^3}{3}.$$

Another calculation gives for the second model

$$a = \sqrt{\frac{3R^2}{7} \frac{7n-5}{3n-1}} \quad \text{and} \quad k = \frac{E\pi R^2}{6nL} \frac{(n-1)(3n-1)}{2n}.$$

## 2.2. Equations of dynamics

Whenever convenient, we will denote by  $q_i$  the  $i$ th coordinate of  $q$ ; the mass matrix  $M(q)$  is defined through the identity

$$T = \frac{\dot{q}^T M(q) \dot{q}}{2},$$

where the superscript  $\top$  denotes the transposition of vectors.

In these generalized coordinates, without constraints, the dynamics of the bar can be written as

$$M(q)\ddot{q} = f(q, \dot{q}). \quad (5)$$

This definition provides us with a consistent mass matrix: the mass matrix is *not* lumped.

Let us consider now the description of the impact. The constraint is

$$y_0 \geq R,$$

and therefore, the set of constraints is

$$K = \{q \in \mathbb{R}^{2n+2} : \phi(q) \geq 0\},$$

where the function  $\phi$  is defined by

$$\phi(q) = y_0 - R = q_2 - R.$$

The generalized impulsion is

$$p = M(q)\dot{q}.$$

Let  $t$  be an instant at which the constraint is active, that is:

$$\phi(q(t)) = 0.$$

The local impact law consists in the transmission of the tangential component of the impulsion and the reflexion of the normal component of the impulsion, which is then multiplied by the restitution coefficient  $e$ . Here, the normal has to be defined in the local metric in the space of impulsions, which can be interpreted in a mathematical sense as the cotangent Riemannian metric at  $q$ ; therefore, the normal component of the impulsion before the impact is

$$p_N(t-0) = \frac{\text{grad } \phi(q)^\top M(q)^{-1} p(t-0)}{\text{grad } \phi(q)^\top M(q)^{-1} \text{grad } \phi(q)} \text{grad } \phi(q).$$

The normal component of the impulsion after impact will be  $-ep_N(t-0)$ , and therefore, the impulsion after impact will be

$$p(t+0) = p(t-0) - (1+e) \times \frac{\text{grad } \phi(q)^\top M(q)^{-1} p(t-0)}{\text{grad } \phi(q)^\top M(q)^{-1} \text{grad } \phi(q)} \text{grad } \phi(q). \quad (6)$$

It is convenient to write our system with constraints as

$$M(q)\ddot{q} = f(q, \dot{q}) + \nu \text{grad } \phi(q), \quad (7)$$

where  $\nu$  is a measure. Indeed we know that the velocities are discontinuous and, from the physical point of view, we expect however the percussions to be finite. Hence, the choice of a reaction belonging to a space of measures therefore makes sense, and all the more since integrals of measures, which are functions of bounded variation, do have limits on the left and on the right. The acceleration will be therefore a (vector-valued) measure and the velocity will be (locally) of bounded variation.

During all the motion,  $q$  is constrained to remain in  $K$ , that is  $\phi(q)$  is non-negative. Writing the reaction as the product of a scalar measure with  $\text{grad } \phi$  expresses that the constraints are perfect; in particular, there is no friction. The measure  $\nu$  is supported in the set of times  $t$  such that  $\phi(q(t))$  vanishes, since there can be no reaction from the constraints if the constraints are inactive. The measure is also non-negative, otherwise there could be an adhesive effect, which is excluded by the perfect constraints assumption.

This information can be abstracted as a complementarity relation

$$0 \leq \phi(q) \perp \nu \geq 0. \quad (8)$$

Here, the orthogonality relation means that the duality product  $\langle \nu, \phi(q) \rangle$  vanishes; this is a product which makes sense if  $\nu$  is a measure and  $\phi(q)$  is a continuous function; by the sign conditions  $\phi(q) \geq 0$  and  $\nu \geq 0$ , if this duality product vanishes, then the measure  $\phi(q)\nu$  vanishes, which implies the support condition as described above.

Of course, we have to add (6)–(8) to obtain a reasonable formulation. Observe indeed that in the cases studied here, all the data are analytic in their arguments. Therefore, Ballard’s uniqueness theorem [14] applies.

We observe moreover that (6)–(8) can be much simplified, since the gradient of  $\phi$  is simply  $e_2$ , the second vector of the canonical basis of  $\mathbb{R}^{2n+2}$ . Let

$$v(q) = M(q)^{-1} e_2, \quad (9)$$

and denote by  $v_i(q)$  the  $i$ th component of  $v(q)$ . With these notations, the transmission law at impact is given for all  $i = 1, \dots, 2n + 2$  by

$$\dot{q}_i(t+0) = \dot{q}_i(t-0) - (1+e) \frac{v_i(q)}{v_2(q)} \dot{q}_2(t-0).$$

For  $i = 2$ , we find

$$\dot{q}_2(t+0) = -e\dot{q}_2(t-0),$$

which is precisely Newton’s law for the impacting degree of freedom.

### 3. The time-stepping scheme

This section is devoted to the description of the theoretical form of the time-stepping scheme; questions of implementation will be treated in Section 4.2.

The rationale for our scheme in the one-dimensional case has been explained in details in [1], and in the multidimensional case, the scheme is given in [2]. Here, we modify slightly these explanations in order to give the linear complementarity problems viewpoint.

After obvious reductions, in the one-dimensional case, with  $K = \mathbb{R}^+$ , we can write our problem as

$$\ddot{q} = f + \nu, \quad (10a)$$

$$0 \leq q \perp \nu \geq 0, \quad (10b)$$

with the impact condition

$$\dot{q}(t+0) = -e\dot{q}(t-0) \quad \text{whenever } q(t) = 0, \quad (10c)$$

or equivalently

$$0 \leq q \perp \ddot{q} - f \geq 0. \quad (11)$$

Problem (11) looks like a classical linear complementarity problem; observe however that its unknown  $q$  is a function and not a finite dimensional vector and that it involves a second differentiation. Nevertheless, there is a simple way of constructing a numerical method out of (11). We replace the second derivative in (11) by a centered finite difference; the approximation of  $q$  must depend on  $q^{n+1}$ ; if we choose  $q^{n+1}$  itself, it is easy to check in the case of a vanishing  $f$  that the solution converges to a limit with vanishing restitution coefficient. A better choice is to approximate  $q$  by  $(q^{n+1} + eq^n)/(1+e)$ , and we have proved in [1] that the restitution coefficient is indeed  $e$  in the limit.

In this case, the linear complementarity problem can be written

$$0 \leq q^{n+1} + eq^{n-1} \perp q^{n+1} - 2q^n + q^{n-1} - \Delta t^2 f^n \geq 0,$$

whose explicit solution is given by

$$q^{n+1} + eq^{n-1} = (2q^n - (1-e)q^{n-1} + \Delta t^2 f^n)^+. \quad (12)$$

The reader is referred to a calculation in [1] which shows that the discrete velocity is reversed and multiplied by  $e$  in two steps when  $f$  vanishes in (12). This calculation also works in the general multidimensional case as shown in [2]. More detailed computations in the one-dimensional case and a comparison with Moreau’s scheme [15,16] and its generalization by Mabrouk [17] can be found in [18].

Eq. (12) is equivalent to

$$\frac{q^{n+1} + eq^{n-1}}{1+e} = P_K \left( \frac{2q^n - (1-e)q^{n-1} + \Delta t^2 f^n}{1+e} \right),$$

where  $P_K$  is the standard projection on the convex set  $K = \mathbb{R}^+$ . In generalized coordinates, the set of admissible positions  $K$  is not necessarily convex anymore. However, for  $q$  in the complement of  $K$  but close enough to  $\partial K$ , there is a unique point  $q' \in \partial K$  which is closest to  $q$  in terms of geodesic distance. Recall that if  $t \mapsto q(t)$  is a path of class  $C^1$  parameterized by  $t \in [0, L]$ , the length of this path is

$$\int_0^L \sqrt{\dot{q}(t)^\top M(q(t)) \dot{q}(t)} dt$$

and the geodesic distance from  $q^0$  to  $q^1$  is the lower bound of all the lengths of paths such that  $q(0) = q^0$  and  $q(L) = q^1$ .

Denote by  $P_K$  this projection according to geodesic distance; then the scheme in dimension  $d$  is defined by

$$q^{n+1} = -eq^{n-1} + (1+e)P_K\left(\frac{2q^n - (1-e)q^{n-1} + \Delta t^2 F^n}{1+e}\right), \quad (13)$$

$$F^n = M(q^n)^{-1}f\left(q^n, \frac{q^{n+1} - q^{n-1}}{2\Delta t}\right). \quad (14)$$

We have defined this numerical method in [1,2], and we have proved its convergence. These are long and technical articles, while the main ideas are described in [19] in a perhaps more accessible format. In particular, we prove that  $q^n$  remains always close to  $K$ . Indeed, by definition of the scheme, the weighted mean  $(q^{n+1} + eq^{n-1})/(1+e)$  always remains in  $K$ ; after proving that the velocity remains bounded independently of the time step, we conclude that  $q^n$  is at most at a distance  $O(\Delta t)$  from  $K$ .

#### 4. From the numerical method to the implementation

In this section, we first describe the implementation of the event-driven method; in particular, we describe the numerical method used when the constraints are inactive and the algorithm used for detecting the impacts. In the second subsection, we describe the modifications that are necessary to make the time-stepping scheme effective; in particular, we replace  $P_K$  by the projection with respect to the frozen metric at  $q^n$  in order to provide an approximate solution of (13), which is precise enough for our purposes.

##### 4.1. Event-driven method

We approximate the motion without constraints (5) by the Newmark's scheme

$$q^{n+1} = q^n + \Delta t w^n + \frac{\Delta t^2}{4}(F^{n+1} + F^n), \quad (15)$$

$$w^{n+1} = w^n + \frac{\Delta t}{2}(F^{n+1} + F^n), \quad (16)$$

where

$$F^n = M(q^n)^{-1}f(q^n, w^n).$$

At each stage, we perform a test: if  $\phi(q^{n+1})$  is non-negative, we continue; if  $\phi(q^{n+1})$  is strictly negative, we seek  $t_{\text{impact}} = t_n + \delta$  such that

$$q_2^n + \delta w_2^n + \frac{\delta^2}{4}(F_2^{n+1} + F_2^n) = R. \quad (17)$$

This is an equation of second degree with respect to  $\delta$ , and we seek the smallest strictly positive root of (17). Then we apply the impact law, and we restart the numerical scheme.

The implementation of the Newmark method demands some numerical caution; we would like to avoid inverting

$M(q^{n+1})$ , since it is implicit in  $q^{n+1}$ . Therefore, we multiply by  $M(q^{n+1})$  (15) and (16), which become

$$M(q^{n+1})(q^{n+1} - A^n) = \frac{\Delta t^2}{4}f(q^{n+1}, w^{n+1}),$$

$$M(q^{n+1})(w^{n+1} - B^n) = \frac{\Delta t}{2}f(q^{n+1}, w^{n+1}).$$

Here  $A^n$  and  $B^n$  are given by

$$A^n = q^n + \Delta t w^n + \frac{\Delta t^2}{4}M^{-1}(q^n)f(q^n, w^n),$$

$$B^n = w^n + \frac{\Delta t}{2}M^{-1}(q^n)f(q^n, w^n),$$

and there is no problem in inverting  $M(q^n)$ , since  $q^n$  is already known: the vectors  $A^n$  and  $B^n$  are known explicitly from the calculation at the previous time step. If we define a transformation  $H_n$  by

$$T = \begin{pmatrix} q \\ w \end{pmatrix}, \quad H_n(T) = \begin{pmatrix} M(q)(q - A^n) - \Delta t^2 f(q, w)/4 \\ M(q)(w - B^n) - \Delta t f(q, w)/2 \end{pmatrix},$$

we have to solve the equation

$$H_n(T) = 0,$$

which we do by a Newton's method, initialized by the values obtained at the previous time step.

##### 4.2. The time-stepping scheme

Let us explain how to implement the time-stepping scheme: there are two difficulties

- (i) we have to approximate  $P_K$  efficiently and
- (ii) the scheme (13), (14) is implicit with respect to  $q^{n+1}$ .

Let us define  $\bar{q}^{n+1}$  by

$$\bar{q}^{n+1} = 2q^n - q^{n-1} + \Delta t^2 M(q^n)^{-1}f\left(q^n, \frac{\bar{q}^{n+1} - q^{n-1}}{2\Delta t}\right). \quad (18)$$

Since the mapping  $(q, v) \mapsto M(q)^{-1}f(q, v)$  is Lipschitz continuous with respect to  $v$ , Eq. (18) admits an unique solution  $\bar{q}^{n+1}$  for  $\Delta t$  small enough and the following alternative holds:

- either  $(\bar{q}^{n+1} + eq^{n-1})/(1+e)$  belongs to  $K$ , and then  $q^{n+1}$  is equal to  $\bar{q}^{n+1}$ ,
- or  $(\bar{q}^{n+1} + eq^{n-1})/(1+e)$  does not belong to  $K$ , and then  $(q^{n+1} + eq^{n-1})/(1+e)$  belongs to  $\partial K$ .

(19)

For this reason, the implementation of scheme (13) and (14) works as follows: we calculate the candidate  $\bar{q}^{n+1}$  by a Newton's method, initialized by the values obtained at the previous time step; we test whether the calculated value of  $(\bar{q}^{n+1} + eq^{n-1})/(1+e)$  belongs to  $K$ . If it belongs to  $K$ , we proceed to next time step; otherwise, we approximate the projection on  $K$  according to the geodesic distance by

the projection on  $K$  with respect to the kinetic metric frozen at  $q^n$ .

It has been proved in the case of a penalty approximation that approximating a geodesic projection by a linear projection relatively to the frozen metric at the point under consideration does not destroy the convergence properties of the method [11]. We expect therefore that it should be possible to retain the convergence properties of the time-stepping numerical scheme when the metric is frozen as described here.

For convenience, we rewrite  $K$  in a fashion that displays the matrix  $M(q^n)$ . Define indeed

$$v^n = \frac{M(q^n)^{-1}e_2}{\sqrt{e_2^T M(q^n)^{-1}e_2}}$$

and

$$s^n = \frac{R}{\sqrt{e_2^T M(q^n)^{-1}e_2}}.$$

Then the condition  $q^T M(q^n)v^n \geq s^n$  is equivalent to

$$\frac{q^T M(q^n)M(q^n)^{-1}e_2}{\sqrt{e_2^T M(q^n)^{-1}e_2}} \geq \frac{R}{\sqrt{e_2^T M(q^n)^{-1}e_2}},$$

proving

$$K = \{q : q^T M(q^n)v^n \geq s^n\}.$$

Then the frozen projection, or projection onto  $K$  with respect to the metric at  $q^n$  is  $P_K^n$ , given by

$$P_K^n q = q + (s^n - q^T M(q^n)v^n)^+ v^n, \quad (20)$$

as can be checked immediately. But there is a simpler form of (20): thanks to the definition of  $v^n$  and  $q^n$ , we may write

$$s^n - q^T M(q^n)v^n = \frac{R - q_2}{\sqrt{e_2^T M(q^n)^{-1}e_2}};$$

with notation (9), we obtain finally

$$P_K^n q = q + \frac{(R - q_2)^+ v(q^n)}{v_2(q^n)}.$$

Instead of solving (13) and (14) we solve

$$q^{n+1} = -eq^{n-1} + (1+e)P_K^n \left( \frac{2q^n - (1-e)q^{n-1} + \Delta t^2 F^n}{1+e} \right),$$

$$F^n = M(q^n)^{-1} f \left( q^n, \frac{q^{n+1} - q^{n-1}}{2\Delta t} \right).$$

The argument working for alternative (19) works with the projection  $P_K$  replaced by the projection  $P_K^n$ ; in particular, if  $(\bar{q}^{n+1} + eq^{n-1})/(1+e)$  does not belong to  $K$ , then  $(q^{n+1} + eq^{n-1})/(1+e)$  belongs to  $\partial K$ . If we write

$$Q^n = \frac{2q^n - (1-e)q^{n-1} + \Delta t^2 F^n}{1+e}, \quad (21)$$

$R - Q_2^n$  is non-negative; therefore, the action of the projection  $P_K^n$  is linear, and we have only to solve

$$q^{n+1} = 2q^n - q^{n-1} + \Delta t^2 F^n + (1+e) \frac{(R - Q_2^n)v(q^n)}{v_2(q^n)}. \quad (22)$$

Observe that (22) is still an implicit equation, since  $F^n$  and  $Q^n$  depend on  $q^{n+1}$ ; but the Lipschitz constant of this dependency is proportional to  $\Delta t^2$ , hence resolution methods will be fast and efficient.

The resolution of (21) and (22) are performed by Newton's method; this resolution is almost the same as that of (18), after obvious changes.

## 5. Quantitative and qualitative results

### 5.1. Conservation of the energy for a restitution coefficient of 1

For a coefficient of restitution  $e = 1$ , we have checked the conservation of the energy, and we have found the results given in Tables 2–5. The expected energy  $W_{\text{exp}}$  is the energy of the model at the initial time, i.e. the kinetic plus the potential energy. Observe that they are slightly different in the event-driven method, where we have used the continuous velocity and in the time-stepping method where we have used the discrete velocity.

We observed that before the first impact, energy is very well conserved; therefore, we considered only the energy after the first impact; its mean is denoted by  $W_{\text{mean}}$ . The relative deviation of the mean is the quotient

$$d_{\text{rel}} = \frac{W_{\text{mean}} - W_{\text{exp}}}{W_{\text{exp}}}. \quad (23)$$

Finally, we give the relative standard deviation of the energy, i.e. the standard deviation of the energy divided by the expected energy

$$s_{\text{rel}} = \frac{\text{standard deviation of the energy}}{\text{expected energy}}. \quad (24)$$

Tables 2–5 show that in any case, the relative deviation of the mean of the energy is less than one percent and the relative standard deviation is at most 0.005. There is no obvious advantage or disadvantage of time-stepping with respect to an event-driven method. Model 2 seems to give a better conservation of energy.

### 5.2. Microimpacts

Let us recall that the height of the constraint  $R$  is the radius of the half-sphere at the impacting tip of the beam; therefore, it is equal to 0.00635 m.

The case of an initial angle of  $90^\circ$  is very special: we observe that there is an interval of contact, after which the beam leaves definitively the obstacle.

This behavior is consistent with the exact analytical solution of the dropped vertical impacting bar, which can be deduced from [20,21]; if we take the vertical downward velocity of the bar to be  $v$ , the velocity of (compression)

Table 2

Conservation of the energy: this table is relative to model 1 and time-stepping

Initial angle	30°	45°	60°	90°
Expected energy, $W_{\text{exp}}$	0.2097923	0.2477831	0.2769345	0.3015103
Maximum of the energy	0.2109452	0.2507776	0.2784425	0.3027040
Minimum of the energy	0.2057284	0.2447674	0.2718261	0.2972322
Relative deviation of the mean, $d_{\text{rel}}$	0.0001307	-0.0033585	0.0042075	0.0080910
Relative standard deviation, $s_{\text{rel}}$	0.0013758	0.0050805	0.0017898	0.0011738

Table 3

Conservation of the energy: this table is relative to model 1 and the event-driven method

Initial angle	30°	45°	60°	90°
Expected energy, $W_{\text{exp}}$	0.2098117	0.2478025	0.2769539	0.3015296
Maximum of the energy	0.2098119	0.2478026	0.2769539	0.3015296
Minimum of the energy	0.2093891	0.2472332	0.2755980	0.2987939
Relative deviation of the mean, $d_{\text{rel}}$	0.0018814	0.0021392	0.0045401	0.0088352
Relative standard deviation, $s_{\text{rel}}$	0.0003568	0.0004093	0.0008881	0.0013079

Table 4

Conservation of the energy: this table is relative to model 2 and time-stepping

Initial angle	30°	45°	60°	90°
Expected energy, $W_{\text{exp}}$	0.2097923	0.2477831	0.2769345	0.3015103
Maximum of the energy	0.2099478	0.2482459	0.2773455	0.3024273
Minimum of the energy	0.2035948	0.2446564	0.2710462	0.2943953
Relative deviation of the mean, $d_{\text{rel}}$	0.0006016	-0.0008674	-0.0005949	0.0042328
Relative standard deviation, $s_{\text{rel}}$	0.0003776	0.0003454	0.0004893	0.0008600

Table 5

Conservation of the energy: this table is relative to model 2 and event-driven method

Initial angle	30°	45°	60°	90°
Expected energy, $W_{\text{exp}}$	0.2098117	0.2478025	0.2769539	0.3015296
Maximum of the energy	0.2099018	0.2479740	0.2770799	0.3015296
Minimum of the energy	0.2097672	0.2476450	0.2766999	0.3014754
Relative deviation of the mean, $d_{\text{rel}}$	-0.0000346	0.0000271	0.0001091	0.0001739
Relative standard deviation, $s_{\text{rel}}$	0.0000837	0.0002058	0.0002774	0.0000293

waves to be  $c$  in the bar and the length of the bar to be  $\ell$ , this analytical solution is

$$u(x, t) = \begin{cases} -vt & \text{if } \max(0, ct) \leq x \leq L, \\ -vx/c & \text{if } ct \leq x \leq 2L - ct, \\ v(t - 2L/c) & \text{if } 2L - ct \leq x \leq L. \end{cases}$$

Here the origin of times is the instant when the bar hits the obstacle.

It is natural to ask whether there exists a numerical method which does not give microimpacts in this special case. If one reduces the problem to a first order equation with a multivalued maximal monotone term, as has been done in [20], no microimpacts are expected. However, this conclusion depends very much on a very precise knowledge of the problem. If we wish to use rather general methods for integrating problems with impact, we cannot hope to have *a priori* this kind of knowledge, and we will be content if, in the vertical case, the microimpacts are very small. This is exactly what we obtained, and the reader is referred to Fig. 4 of the supplement at <http://math.univ-lyon1.fr/~schatz/beamsimu.html>.

For other angles, there is first a very similar interval of contact, with slightly larger microbounces, after which the beam leaves the obstacle (see Fig. 3); depending on the initial angle, the beam hits again or does not hit again (see Fig. 4). The reason for this behavior is that the flexion modes are excited; if the initial angle is large enough, then the flexion oscillations of the beam are not large enough to cause secondary contact intervals.

Since the microimpacts have been observed by Stoianovici and Hurmuzlu [3], our method should give them, and indeed it does.

The computations were performed on a PC Pentium 4, 1.8 GHz, 256 MRam. A comparison of the CPU times (see Fig. 3) shows that the time-stepping scheme is almost 40% faster than the event-driven method.

### 5.3. Apparent coefficient of restitution

In order to obtain concrete results, we calculated an apparent coefficient of restitution. For this purpose, we averaged the vertical velocity of the impacting degree of freedom, i.e.  $\dot{q}_2$  over a time interval of 0.00250 s after the last microbounce. We have chosen this time interval because we thought that the outgoing velocity after the last impact might be irregular; this choice is larger than Hurmuzlu's averaging over one millisecond. The averaging process reflects the behavior of measuring instruments, which never give a precisely instantaneous velocity.

Results are obtained for the event-driven method and the time-stepping scheme and for the two models considered here: they are displayed in Fig. 5. On each picture, five different values of  $e$  are represented, namely (a)  $e = 1$ , (b)  $e = 0.75$ , (c)  $e = 0.50$ , (d)  $e = 0.25$  and (e)  $e = 0$ .

For comparison purposes, we display at Fig. 6 an analogous set of results for model 2 and time-stepping, with an averaging over one millisecond.

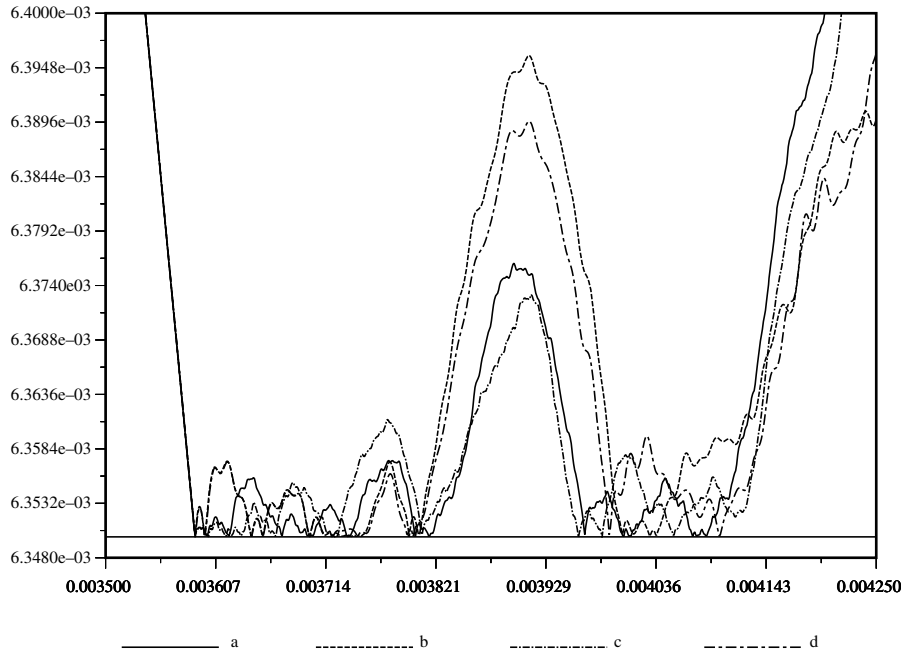


Fig. 3. The dynamics of the center of the half-sphere at the tip of the beam (coordinate  $q_2$ ) for an initial angle of  $30^\circ$  relatively to the horizontal; the two models and the two methods are represented here: (a) event-driven, model 1; (b) event-driven, model 2; (c) time-stepping, model 1; (d) time-stepping, model 2. CPU times: (a) 66.755 s; (b) 78.148 s; (c) 46.061 s; (d) 53.279 s.

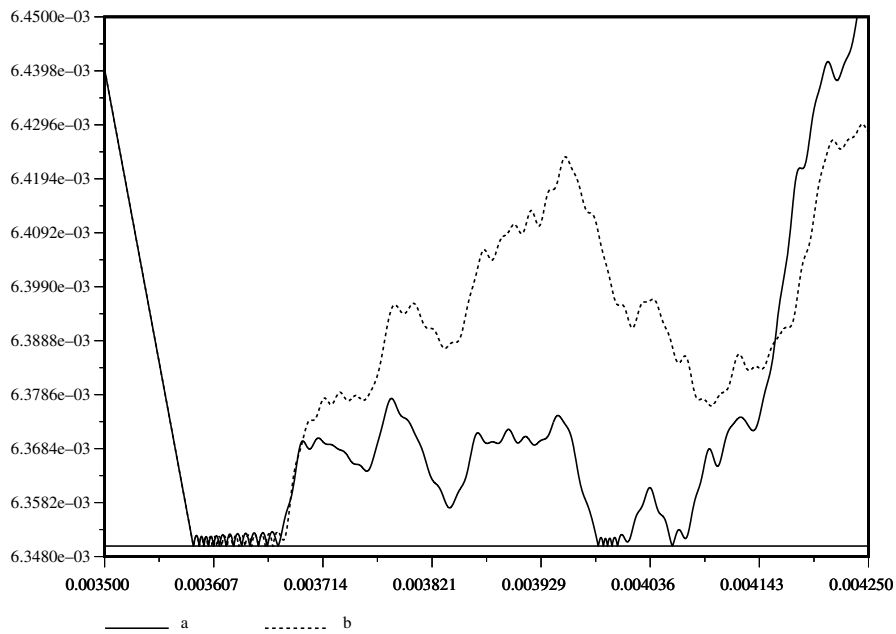


Fig. 4. For initial angles of (a)  $65^\circ$  and (b)  $70^\circ$ , the beam has different behaviors; the computation displayed here is for time-stepping and model 2.

We could not enclose all the relevant figures in the present article, and the reader is referred to the web page <http://maply.univ-lyon1.fr/~schatz/beamsimu.html> for a wealth of extra results, in color and with much more information.

The dip in the curve, which can be seen very stably on all the figures, corresponds to the transition from a situation where there is only one contact interval to a situation where

there is more than one, as observed and then analyzed first in [3,4], and then justified mathematically in [5].

We have determined theoretically in [5] a condition under which this secondary contact interval appears. See Fig. 7 for a comparison between the apparent coefficient restitution as calculated in [5] and by the present calculations.

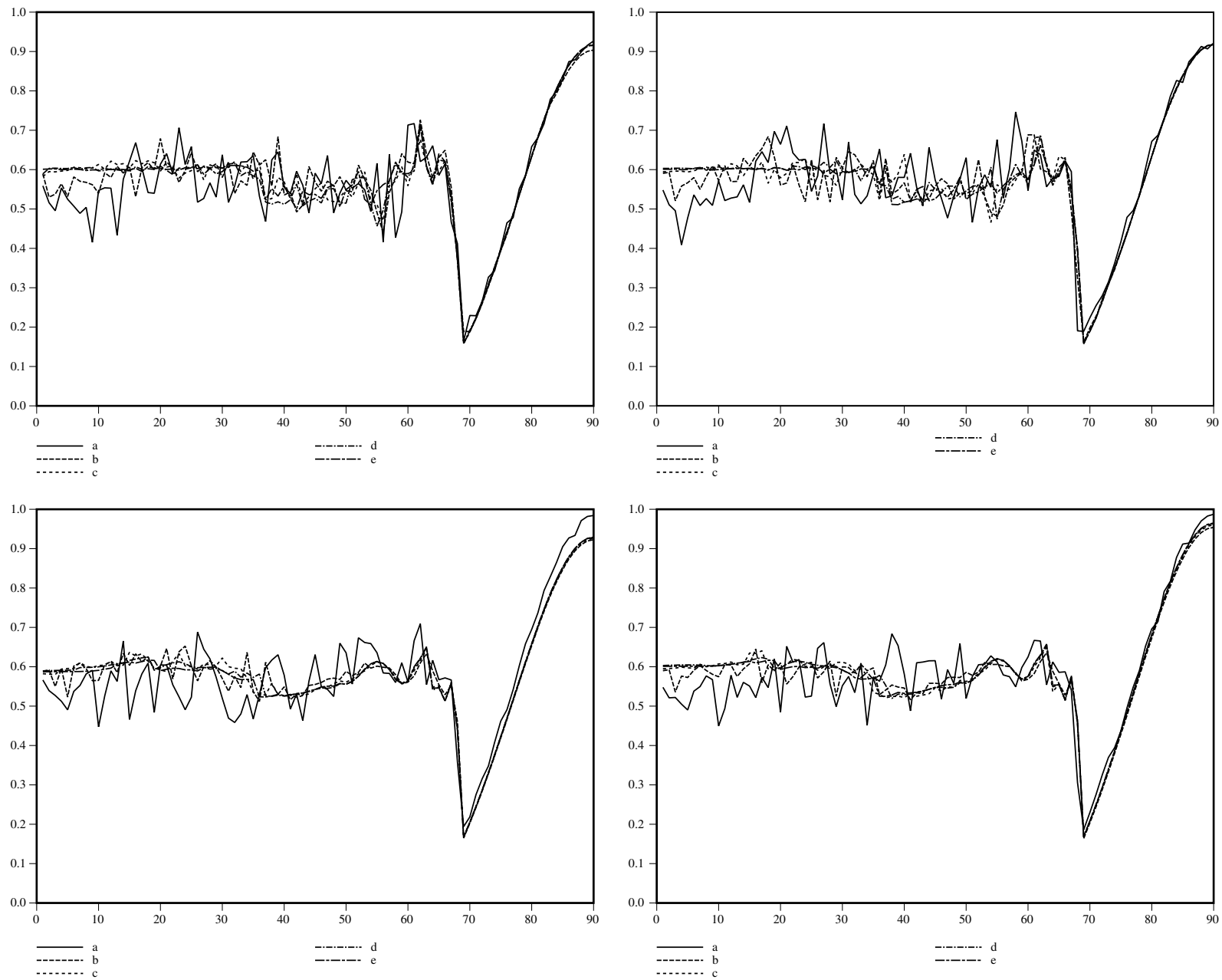


Fig. 5. The apparent coefficient of restitution as a function of the initial angle, for (a)  $e = 1$ , (b)  $e = 0.75$ , (c)  $e = 0.50$ , (d)  $e = 0.25$  and (e)  $e = 0$ . Top left: model 1, event-driven; bottom left: model 2, event-driven; top right: model 1, time-stepping; bottom right: model 2, time-stepping.

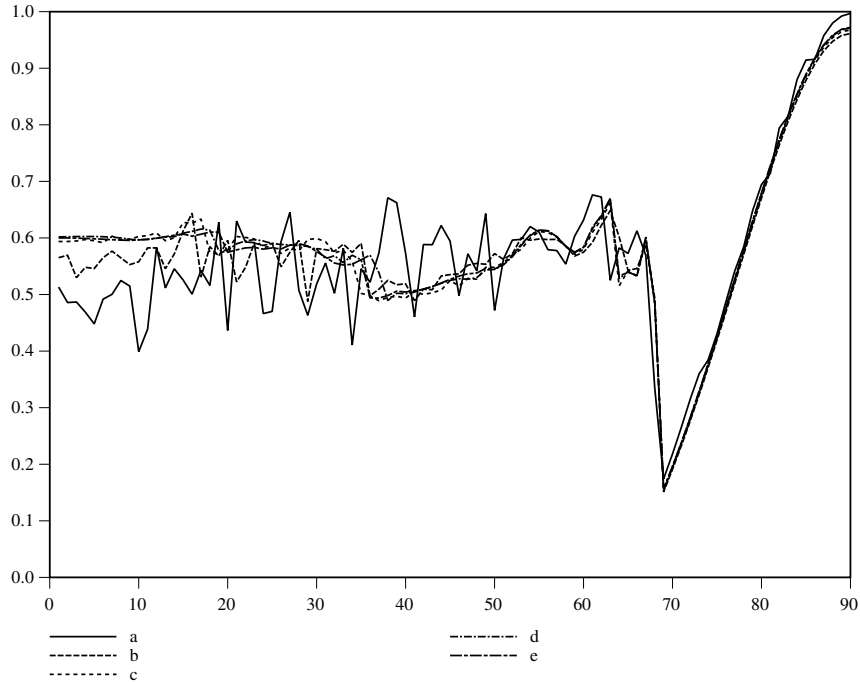


Fig. 6. The present figure corresponds to the same choice of parameters as the bottom right figure in Fig. 5, save for the averaging time, which is  $10^{-3}$  s, as in Stoianovici and Hurmuzlu [3].

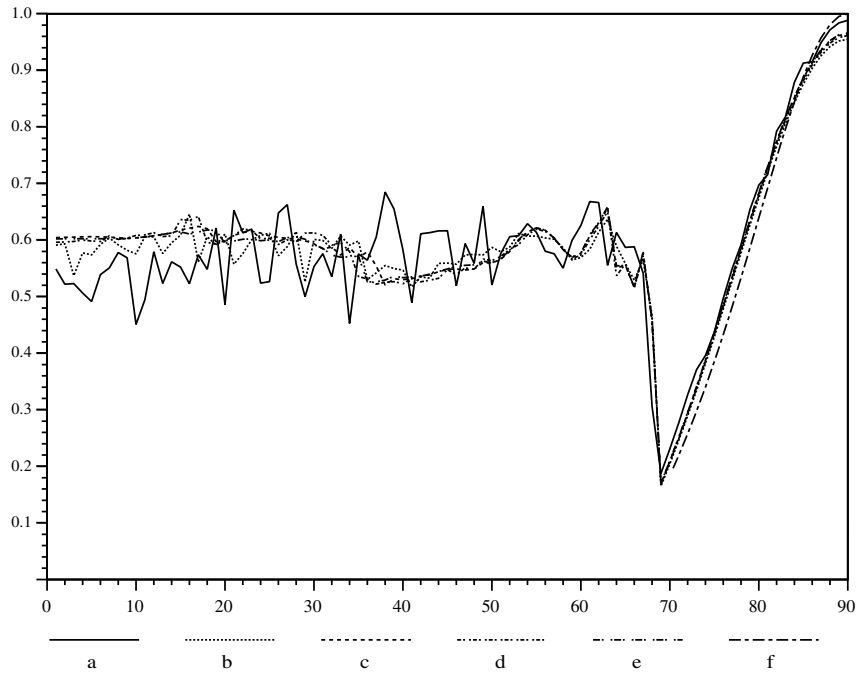


Fig. 7. Comparison between the calculation of the apparent restitution of coefficient for the time-stepping scheme and model 2 (a)  $e = 1$ , (b)  $e = 0.75$ , (c)  $e = 0.5$ , (d)  $e = 0.25$ , (e)  $e = 0$  and (f), the theoretical prediction from [5].

#### 5.4. Non-equilibrium initial data

In order to estimate the influence of very small uncertainties on the initial data, we simulated the same problem assuming that the beam was not initially at equilibrium.

Initially, the beam is excited along its discrete first eigenmode, with an energy which is a fraction  $\eta$  of the total ini-

tial kinetic energy; the phase of the initial excitation varied from  $0^\circ$  to  $180^\circ$  by intervals of  $20^\circ$ . The simulation whose results are shown in Figs. 8 and 9 emphasize that the dip is still there, very stably. However, what goes on for angles smaller than the abscissa of the dip displays a very chaotic situation, which depends strongly on the coefficients  $\eta$  and  $e$ .

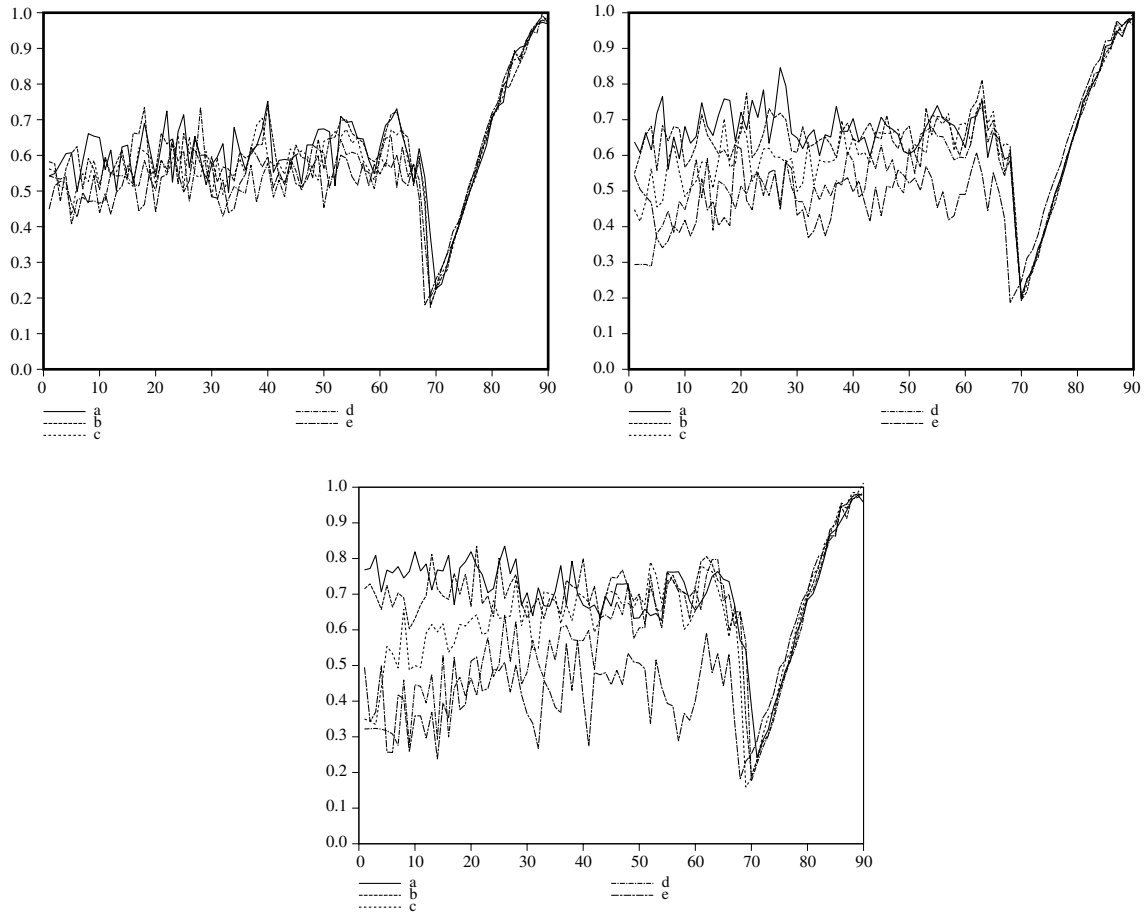


Fig. 8. Model 2, time-stepping, three different levels of relative energy of the perturbation:  $\eta = 10^{-3}$ ,  $\eta = 5 \times 10^{-3}$  and  $\eta = 10^{-2}$ , from left to right and from top to bottom. The restitution coefficient is  $e = 1$  and the phase of initial excitation is (a)  $0^\circ$ , (b)  $40^\circ$ , (c)  $80^\circ$ , (d)  $120^\circ$  and (e)  $160^\circ$ .

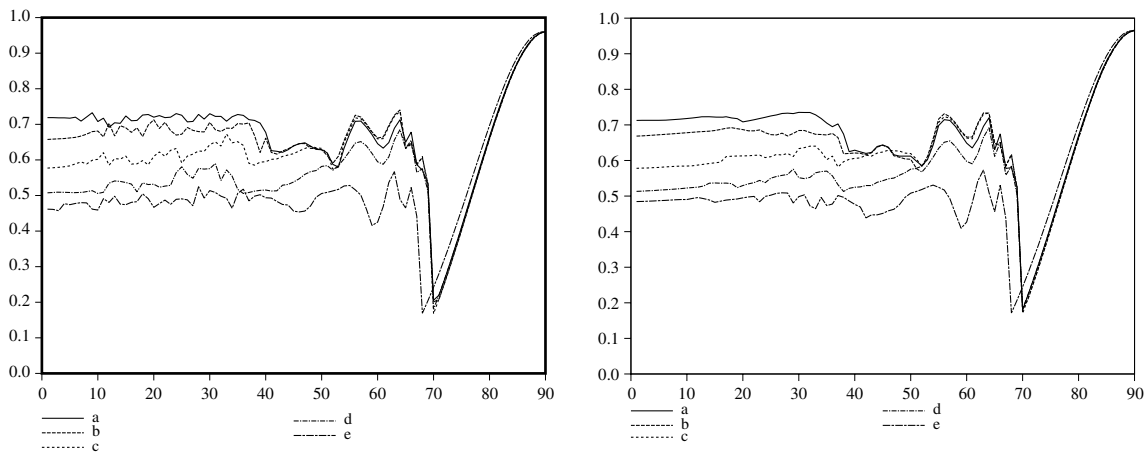


Fig. 9. Model 2, time-stepping,  $\eta = 5 \times 10^{-3}$ ,  $e = 0.5$  and  $e = 0$  from left to right. Same conventions as above.

This is a question that had been asked by David Stewart in his article [22], who wondered whether the phase in the initial data might have an influence on the behavior of the beam. The answer is twofold: for angles larger than the abscissa of the dip, there is almost no influence, and

for angles below this critical abscissa, the influence is very important, and depends on the coefficients  $\eta$  and  $e$ .

There are qualitative differences for different values of  $e$ , but they do not affect what is going on for angles larger than the critical abscissa.

## 6. Conclusion

The time-stepping scheme described here converges, according to our work [1,2]; we have shown that it can be implemented without difficulty and that it gives results which compare well with experiments. Moreover, the different numerical methods and models agree together and with the asymptotics from [5].

The notion of restitution coefficient does not make much sense when continuous medium vibrations are present, and its value has little influence on the final results. We believe that the influence of the value of  $e$  tends to 0 as the discretization becomes finer, but we have not confirmed this statement numerically.

## References

- [1] L. Paoli, M. Schatzman, A numerical scheme for impact problems. I. The one-dimensional case, *SIAM J. Numer. Anal.* 40 (2) (2002) 702–733 (electronic).
- [2] L. Paoli, M. Schatzman, A numerical scheme for impact problems II. The multidimensional case, *SIAM J. Numer. Anal.* 40 (2) (2002) 734–768 (electronic).
- [3] D. Stoianovici, Y. Hurmuzlu, A critical study of the applicability of rigid body collision theory, *ASME J. Appl. Mech.* 63 (1996) 307–316.
- [4] Y. Hurmuzlu, An energy based coefficient of restitution for planar impacts of slender bars with massive external surfaces, *ASME J. Appl. Mech.* 65 (1998) 952–962.
- [5] L. Paoli, M. Schatzman, Understanding impact through continuous medium vibrations, in: J. Martins, M. Monteiro-Marques (Eds.), *Contact Mechanics*, no. 103 in *Solid Mechanics and its Applications*, Kluwer, 2002.
- [6] W.J. Stronge, *Impact Mechanics*, Cambridge University Press, 2000.
- [7] L. Paoli, M. Schatzman, Dynamics of an impacting bar, in: W. Wunderlich, (Ed.), *Proceedings of European Conference on Computational Mechanics*, Munich, 1999 (CD-ROM).
- [8] M. Schatzman, A class of nonlinear differential equations of second order in time, *Nonlinear Anal.: Theory, Methods Appl.* 2 (1978) 355–373.
- [9] L. Paoli, M. Schatzman, Mouvement à un nombre fini de degrés de liberté avec contraintes unilatérales: cas avec perte d'énergie, *Modél. Math. Anal. Num. (M2AN)*.
- [10] M. Panet, L. Paoli, M. Schatzman, Theoretical and numerical study for a model of vibrations with unilateral constraints, in: M. Raous, M. Jean, J.-J. Moreau (Eds.), *Contact Mechanics*, Plenum Press, 1995, pp. 457–464.
- [11] M. Schatzman, Penalty method for impact in generalized coordinates, *Phil. Trans. R. Soc. Lond.* 359 (1789) (2001) 2429–2446.
- [12] L.A. Paoli, An existence result for vibrations with unilateral constraints: case of a nonsmooth set of constraints, *Math. Models Methods Appl. Sci.* 10 (6) (2000) 815–831.
- [13] L. Paoli, M. Schatzman, Ill-posedness in vibroimpact and its numerical consequences, in: *Proceedings of European Congress on Computational Mechanics*, 2000 (CD-ROM).
- [14] P. Ballard, The dynamics of discrete mechanical systems with perfect unilateral constraints, *Arch. Rat. Mech. Anal.* 154 (2000) 199–274.
- [15] J.-J. Moreau, *Unilateral Problems in Structural Analysis*, no. 288 in *CISM Courses and Lectures*, Springer, Ch. *Standard Inelastic Shocks and the Dynamics of Unilateral Constraints*, 1985.
- [16] J.-J. Moreau, *Dynamique des systèmes à liaisons unilatérales avec frottement sec éventuel; essais numériques*, Tech. Rep. 85, LMGC, Université des Sciences et Techniques du Languedoc, 1986.
- [17] M. Mabrouk, A unified variational model for the dynamics of perfect unilateral constraints, *Eur. J. Mech. A Solids* 17 (5) (1998) 819–842.
- [18] L. Paoli, Time-discretization of vibro-impact, *Phil. Trans. Roy. Soc.* 359 (1789) (2001) 2405–2428.
- [19] L. Paoli, M. Schatzman, Approximation et existence en vibro-impact, *C.R. Acad. Sci. Paris Série I* 329 (1999) 1103–1107.
- [20] M. Schatzman, Un problème hyperbolique du 2ème ordre avec contrainte unilatérale: la corde vibrante avec obstacle ponctuel, *J. Differ. Equat.* 36 (2) (1980) 295–334.
- [21] M. Schatzman, M. Bercovier, Numerical approximation of a wave equation with unilateral constraints, *Math. Comp.* 53 (187) (1989) 55–79.
- [22] D.E. Stewart, Rigid-body dynamics with friction and impact, *SIAM Rev.* 42 (1) (2000) 3–39 (electronic).